SAR Distribution in a Bio-Medium in Close Proximity with Dual Segment Rectangular Dielectric Resonator Antenna

Ravi Kumar Gangwar[1], S. P. Singh[1], D. Kumar[2]

[1]Department of Electronics Engineering, Institute of Technology, Banaras Hindu University, Varanasi-221005, Uttar Pradesh, India, Email: ravi.gangwar.ece07@itbhu.ac.in; phone: +91 542 6701258

[2]Department of Ceramic Engineering, Institute of Technology, Banaras Hindu University, Varanasi-221005, Uttar Pradesh, India

Abstract: In this paper, the simulation and experimental studies of SAR distribution in a bio-medium in close proximity with dual segment rectangular dielectric resonator antenna (DSRDRA) in C-band of microwave frequencies are reported. The simulation study has been carried out using CST Microwave Studio software. The experimental results for SAR distribution are compared with simulated results.

Index Terms: DSRDRA, Return loss, SAR and muscle layer

I. INTRODUCTION

The use of wireless portable devices is growing at fast rate throughout the world. These devices are often used in the vicinity of human body. The continuous growth of wireless portable devices has prompted the researchers to study the interaction between the electromagnetic waves emanating from the device antenna and the human body. These studies are motivated by two factors; first one stems from the need to evaluate the performance of antenna in terms of parameters like return loss and bandwidth in presence of bio-medium, and the second factor is concerned with the rate of electromagnetic energy absorption, known as specific absorption rate (SAR) [1]. The human body, being lossy, absorbs certain amount of electromagnetic radiation generated from portable wireless device situated in its vicinity. Therefore, it is of interest to evaluate the power absorbed /specific absorption rate (SAR) distribution in the body tissues due to wireless device antenna radiating electromagnetic waves [2]. The electric field induced and hence SAR within the human body depends on several factors including the strength and frequency of the external field, the shape, size and electrical characteristics of the body tissues and the orientation of the body in relation to the external field.

Dielectric Resonator Antennas (DRAs) are considered as one of the most suitable antenna structures for these applications due to their low profile, flexible feed arrangement, high radiation efficiency, large bandwidth, wide range of material dielectric constants, ease of excitation, easily controlled characteristics and ease of integration with other active or passive microwave integrated circuit (MIC) components [3-7]. The methods used to improve the bandwidth of the DRAs include changing the aspect ratio of DRA, employing multi-segments and stacked DRAs and by varying the dielectric constant of DRA material. For wider-band applications, DRAs having lower dielectric constant values are preferred. This results in week coupling. Multi-segment DRAs can be used to overcome this problem [8-9].

Only a few studies are reported in the literature on SAR distribution in bio-tissues due to DRAs radiating electromagnetic waves. The FDTD method has been applied for computing SAR distribution inside the human head, and the effects of the human proximities including the head, the hand, and the user's glasses on the antenna performance have been analyzed [10]. Off-centre ring DRA has been designed and also used for evaluation of SAR distribution in human head [11]. The performance of rectangular DRA (RDRA) in close proximity with the user's body was studied with the help of user's hand model [12]. A few simulation and experimental studies on SAR distributions in a bio-media/bio-medium due to DRAs at microwave frequencies have also been reported in the literature [13-16].

This paper provides simulation and experimental investigations of SAR distribution in a bio-medium in close proximity with dual segment rectangular DRA in C-band of microwave frequencies. The simulation study has been carried out using CST Microwave Studio software. The measurement of power levels proportional to square of the magnitude of induced electric field components in the artificial muscle medium and hence SAR distribution in the medium has been performed with the help of Agilent make Spectrum analyzer in C-band of microwave frequencies. The simulated results for SAR distribution are compared with experimental results.

II. ANTENNA GEOMETRY AND PHANTOM MUSCLE LAYER

The proposed dual segment RDRA consists of a lower segment of Teflon sheet with dielectric constant $\varepsilon_{r1} = 2.1$ and loss tangent tan δ = 0.0004, and an upper segment of alumina block with $\varepsilon_{r2} = 9.8$ and tan δ = 0.0001 respectively as shown in Fig. 1. A rectangular coordinate system with the Z-axis oriented along the axis of the DSRDRA and perpendicular to the ground plane, and the X-Y plane parallel to ground plane as well as top and bottom circular surfaces of DSRDRA has been considered. The DSRDRA is placed on a ground plane of size 60×60×4 mm^3. The lower and upper segments of the DRA have dimensions of $a \times b \times$l and $a \times b \times l_1$ respectively. The DRA is excited by a 50 Ω coaxial probe of outer radius 2 mm and inner radius 0.6 mm. The design parameters of the antenna are: a = 20 mm, b = 12 mm, l = 10 mm, l_1 = 3 mm and probe height = 11.6 mm.

For an RDRA of dimensions $a \times b \times$h, the lowest order mode is $TE^{y}_{1\delta 1}$ mode. The resonant frequency for $TE^{y}_{1\delta 1}$ mode of RDRA is calculated by solving the following equations [8]:

$$k_y \tan\left(\frac{k_y b}{2}\right) = \sqrt{k_x^2 + k_z^2 - k_0^2} \qquad (1)$$

$$k_x^2 + k_z^2 + k_z^2 = k_0^2 \varepsilon_r \qquad (2)$$

where k_0 denotes the free space wave number corresponding to the resonant frequency and k_x, k_y and k_z denote the wave numbers along the x-, y- and z-directions respectively. Wave numbers k_0, k_x and k_z are determined by the following relation:

$$k_0 = \frac{2\pi}{\lambda_0} = \frac{2\pi\ f_o}{c}\ ,\ \ k_x = \frac{m\pi}{a}\ \ \ k_z = \frac{l\pi}{2h}$$

For given resonator parameters ε_r, a, b, and h the resonant frequency of DRA is the one at which wave number k_y satisfies equations (1) and (2). The resonant frequency f_o can be written as

$$f_o = \frac{c}{2\pi\sqrt{\varepsilon_r}}\sqrt{k_x^2 + k_y^2 + k_z^2} \qquad (3)$$

Radiation Q-factor of RDRA can be written as [8]

$$Q = \frac{2\omega_0 W_e}{P_{rad}} \qquad (4)$$

where W_e and P_{rad} are respectively the stored energy and radiated power of the RDRA and $\omega_0 = 2\pi\ f_o$ is the resonant angular frequency of the antenna. The stored energy W_e and radiated power P_{rad} are given by

$$W_e = \frac{\varepsilon_r \varepsilon_0 abhA^2}{32}\left(1 + \frac{\sin(k_y b)}{k_y b}\right)\left(k_x^2 + k_z^2\right)$$

and

$$P_{rad} = 10 k_0^4 \left|p_m\right|^2$$

where , p_m is the magnetic dipole moment of the RDRA:

$$p_m = \frac{-j8\omega\varepsilon_0(\varepsilon_r - 1)A}{k_x k_y k_z}\sin\left(\frac{k_y b}{2}\right)$$

and A is an arbitrary constant related to the maximum amplitude of the fields.

The percentage bandwidth of RDRA is given by [8]

$$\%BW = \frac{s-1}{Q\sqrt{S}} \times 100 \qquad (5)$$

where S is the VSWR of RDRA.

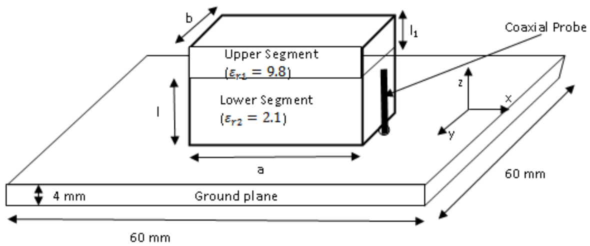

(a)

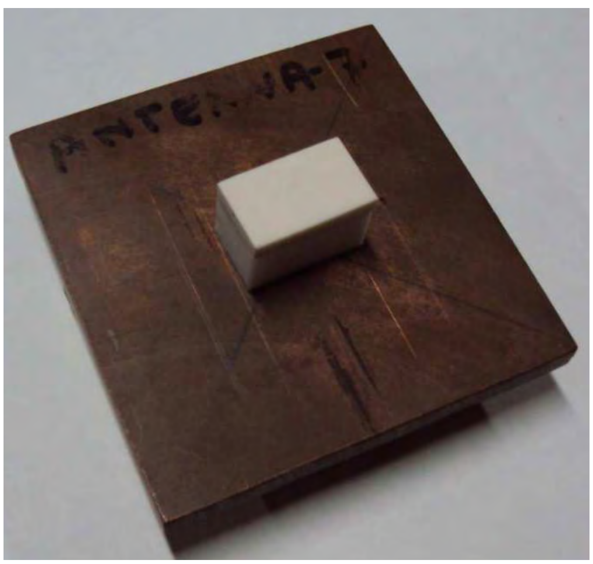

Fig.1 Antenna Geometry (a) Layout, (b) Fabricated Structure

Equations (3)-(5) can respectively be used to compute the resonant frequency, radiation Q-factor and bandwidth of the dual segment RDRA by replacing RDRA material dielectric constant, ε_r and height h with their modified parameters termed as ε_{eff} and h_{eff} respectively. Adopting a simple static capacitance model, the following expression for ε_{eff} and h_{eff} are obtained:

$$\varepsilon_{eff} = \frac{h_{eff}}{\frac{1}{\varepsilon_{r1}} + \frac{1}{\varepsilon_{r2}}} \text{, and } \quad h_{eff} = l + l_1 \qquad [8], [17]$$

where l and l_1 are the length of lower and upper segments of RDRA respectively.

The resonant frequency, Q-factor and bandwidth of the DSRDRA computed using equations (1), (2) and (3) are found to be 5.06 GHz, 3.8706 and 18.26% respectively.

The phantom muscle was prepared from the material composition given in reference [18] i.e., an aqueous solution of sucrose ($C_{12}H_{22}O_{11}$, 1.0 mol/l). The phantom muscle medium is prepared by mixing double distilled water with highly pure laboratory grade sucrose powder (obtained from Qualigens Fine Chemicals Pvt. Ltd, India). The permittivity of the artificial muscle-model is assumed to be 53.01, 52.012 and 50.454 at 4.7 GHz, 5.2 GHz and 5.63 GHz respectively [18]. The electric conductivity of the muscle is assumed to 3.7214, 4.2669 and 4.7606 S/m at 4.7 GHz, 5.2 GHz and 5.63 GHz respectively. The phantom muscle was contained in one part of a chamber of inner dimensions 15 cm × 15 cm × 15 cm fabricated using Perspex sheet of thickness equal to 4 mm. The Perspex chamber shown in Fig. 5 has been divided into two parts. One part contains the sucrose solution and is separated from the other part housing the antenna by miler sheet of thickness 0.2 mm.

III. SIMULATION OF DSRDRA INPUT CHARACTERISTICS AND SAR DISTRIBUTION IN PHANTOM MUSCLE

The theoretical analysis involved in the design of some antennas can become quite complex and in many cases an exact solution may not be possible. CST Microwave Studio is the powerful and easy-to-use electromagnetic field simulation software, based on Finite Integration Method.

Simulation of input characteristics of RDRA in free space and in presence of phantom muscle layer and SAR distribution in the phantom muscle layer due to the antenna was carried out using CST Microwave Studio software. The input characteristics of the antenna include the variations of return loss and VSWR versus frequency and the values of input resistance at resonance with and without phantom muscle.

For simulating the structure wave port mode of excitation was used for the coaxial feed and the radiation boundary was fixed at a distance of λ/4, λ being the free space wavelength corresponding to the lowest component of the frequency sweep. The solver accuracy of -30dB was used which limits the truncation error down to one percent. Transient domain solver has been employed to generate the results. Maximum S-parameter value of 0.02 was chosen for terminating the adaptive solution as this gives reasonably accurate simulation results.

IV. RESULTS AND DISCUSSION

A. Return Loss Versus Frequency Characteristics

The return loss of DSDRA in free space and in presence of phantom muscle layer were measured at different frequencies over 4.0 – 7.0 GHz range using Agilent PNA series Vector Network Analyzer (Model No. E8364B). The measured and simulated variations of return loss as functions of frequency for the DSRDRA in free space and in the presence of phantom muscle layer when it is separated from the antenna by miler sheet of thickness equal to 0.2 mm is shown in Fig. 2. From Fig. 2 the resonant frequency and percentage bandwidth of the proposed DSRDRA in free space are extracted and the results are shown in Table 1. From Table 1, it can be observed that the measured resonant frequency of antenna in free space is nearly in agreement with theoretical and simulated values. The experimental bandwidth of antenna in free space deviates from theoretical/simulated values. The deviation in the results may be due to fabrication tolerances, the possibility of misalignment in the placement of two DRA segments, effect of finite size ground plane not considered in theoretical computation, and the effect of glue used to bind the two DRA segments during fabrication of antenna.

From Fig. 2 it can be seen that measured resonant frequency of DSRDRA in presence of synthetic muscle is 4.7 GHz, which is 25 MHz more than the resonant frequency of antenna in free space. Also, the simulated resonant frequency in the presence of phantom muscle is 4.948 GHz, which is 231 MHz higher than the resonant frequency of antenna in free space. The increase in resonant frequency in the presence of muscle layer may be attributed to more concentration of energy in the lower segment having lower dielectric constant as compared to that in the upper segment (Fig. 3), which has caused the reduction in effective dielectric constant of the antenna materials in presence of bio-medium. This effect has given rise to perturbation in the resonant mode and near field distribution for $TE^{y}_{1\delta 1}$ mode as shown in Fig. 3. From Fig. 2 it can be observed that the values of input VSWR of the DSRDRA in presence of the phantom muscle are higher than the corresponding parameter values of antenna in free space. This may be attributed to wave reflections due to abrupt changes in the medium when antenna is in the vicinity of the bio-medium.

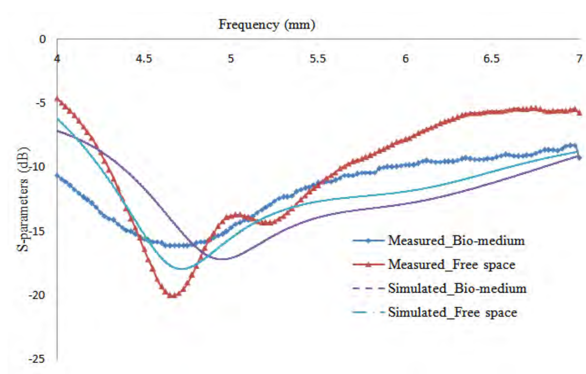

Fig. 2 Return loss versus frequency characteristics of DSRDRA

Table 1 Return loss parameters of DSRDRA in free space

Parameters	Resonant Frequency	% Bandwidth
Theoretical	5.06 GHz	18.27
Measured	4.675 GHz	28.89
Simulated	4.717 GHz	49.52

B. Near Field Distribution

The simulation study of field distribution in the proposed DSRDRA in free space and in close proximity with bio-medium has been carried out at the resonant frequency 4.717 GHz, of antenna in free space using CST Microwave Studio software. When DSRDRA is excited using 50 Ω coaxial probe as shown in Fig. 1, the electric field distributions shown in Fig. 3 are obtained. It is apparent from Fig. 3 (a) that the coaxial probe excites $TE^{y}_{1\delta 1}$ dominant mode fields within the DSRDRA in free space. This dominant mode is excited within the DSRDRA terminated in free space. The mode of operation and field distribution are disturbed when the bio-medium is placed in the vicinity of the antenna Fig. 3 (b). The deviation in field distribution may be due to the reflections/scattering caused by abrupt changes in the media.

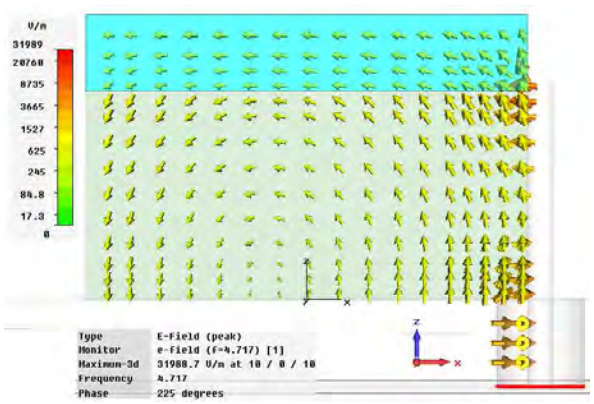

(a)

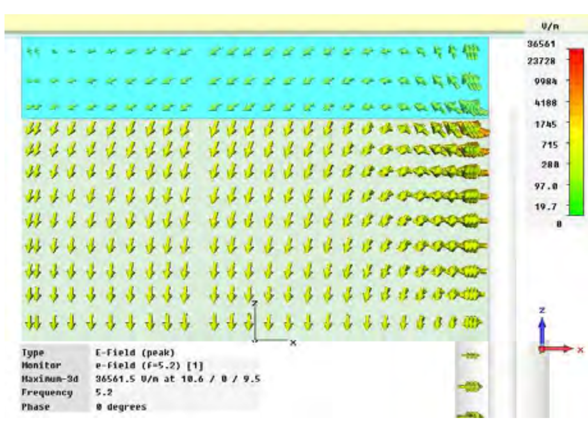

(b)

Fig. 3 Near Field distribution of DSRDRA (a) in free space, (b) in bio-medium

C. Far Field Distribution

The simulated radiation patterns of the DSRDRA in free space as well as in close proximity with phantom muscle at respective resonant frequencies are given in Fig. 4. From Fig. 4, it can be observed that the presence of phantom muscle distorts the radiation patterns as compared to those in free space.

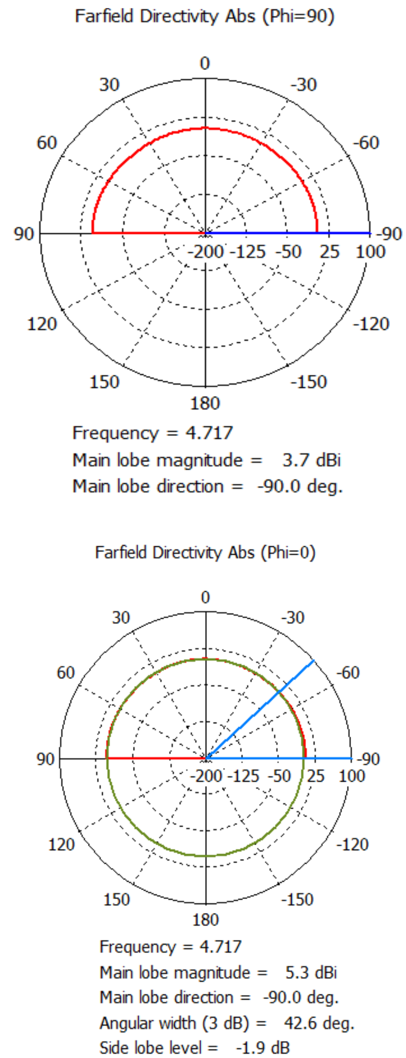

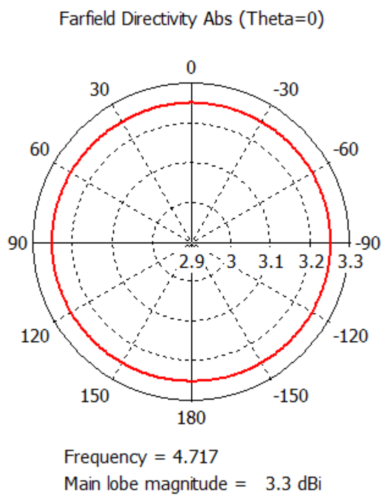

(a)

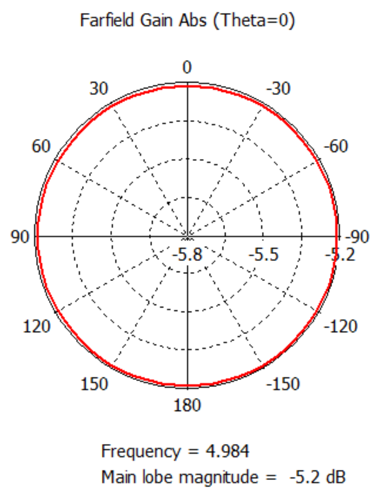

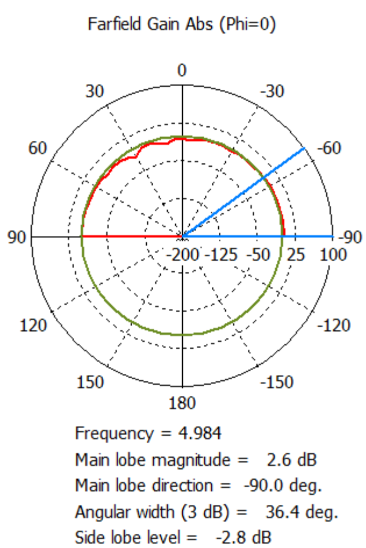

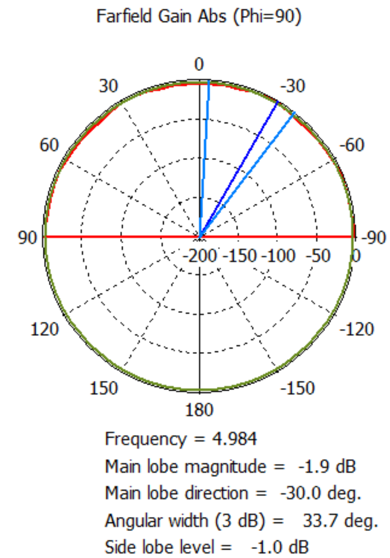

(b)

Fig. 4 Radiation pattern of DSRDRA (a) in free space, (b) in presence of phantom muscle

V. EXPERIMENTAL TECHNIQUE FOR DETERMINATION OF SAR DISTRIBUTIONS IN PHANTOM MUSCLE LAYER

The experimental setup for measuring the power levels proportional to square of electric field components in artificial muscle-medium separated from DSRDRA by miler sheet of thickness equal to 0.2 mm to DSRDRA is shown in Fig. 5. The procedure for experimental determination of SAR distribution in artificial muscle layer due to the antenna is the same as that given in reference [15]. The measured power levels proportional to square of components of induced electric field have been used to determine SAR-distributions in the phantom muscle at the measured resonant frequency of 4.7 GHz (in the presence of muscle layer) and at two other frequencies 5.2 GHz (in 5.15-5.35 GHz low & mid U-NII band) and 5.63 GHz (in 5.47-5.725 GHz WRC band). The values of specific absorption rate (SAR) in phantom muscle medium were computed with the help of the following formula:

$$SAR = \frac{\sigma |E|^2}{2\,\rho} \tag{7}$$

where $|E|$ is the magnitude of total electric field intensity in the bio-medium, σ and ρ are respectively the conductivity and density of the bio-medium. The muscle density of 1050 Kg/m^3 was used in the computation [19].

The accuracy in the measurement of distance along X-/Y-/Z- directions is 1 mm. The error in measurement of power level (proportional $|E_x|^2$ / $|E_y|^2$/$|E_z|^2$) is ± 0.01 dB. Although the probe position could not be measured to the degree of accuracy required for precision measurements, it was sufficient to prove the feasibility of this technique.

The experimental SAR distribution in the artificial muscle due to DSRDRA is shown in Figure 6.

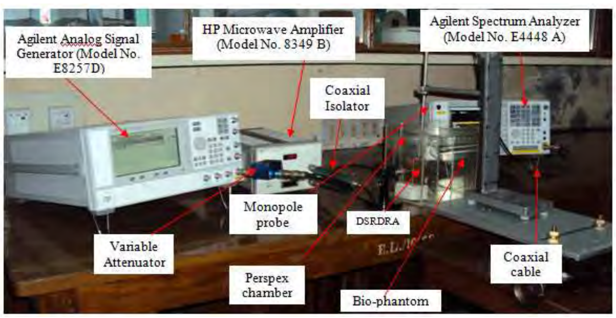

Fig. 5 (a) Experimental setup for electric field intensity measurement

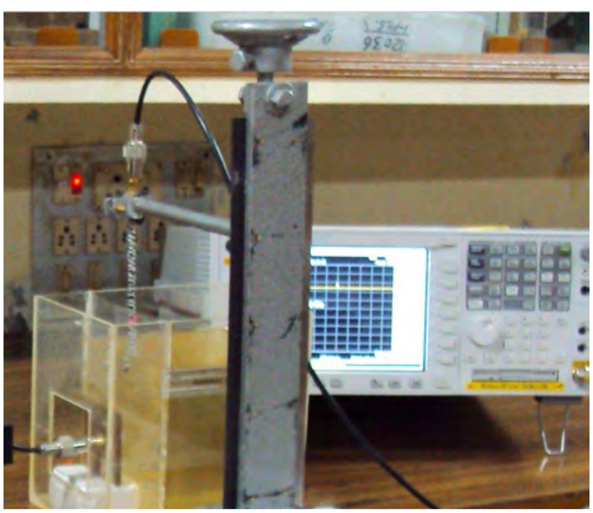

Fig. 5 (b) Expanded view of a part of the setup including phantom muscle and coaxial monopole probe

VI. SIMULATED SAR DISTRIBUTION

The relative SAR distribution in phantom muscle medium (120×120×150 mm^3) in close proximity with the proposed DSRDRA at the measured resonant frequency of 4.7 GHz and at other frequencies 5.2 GHz (in 5.15-5.35 GHz low & mid Unlicensed National Information Infrastructure (U-NII) band), 5.63 GHz (in 5.47-5.725 GHz World Radio Conference (WRC) band) were determined through simulation using CST Microwave Studio software. The simulated SAR distributions are shown in Fig. 6.

VII. COMPARISON OF SIMULATED AND EXPERIMENTAL SAR DISTRIBUTIONS

The simulated and experimental SAR distributions in the synthetic muscle due to DSRDRA are compared at the measured resonant frequency of 4.7 GHz and at 5.2 GHz and 5.63 GHz (Fig. 6).

From Fig. 6, it can be observed that experimental SAR values are deviating to a small degree from corresponding simulated values. This deviation may be due to the measured resonant frequency of 4.7 GHz not matching exactly with the simulated value and error in measuring the position of the monopole probe which affects the accuracy of measured results. Interaction between the probe and the DSRDRA may also occur. Although, these factors could cause negligible effect on SAR-value independently but taken collectively may become significant and cause the mismatch between simulated and experimental SAR values. From Fig. 6 it may be noted that measured SAR distribution in X-direction is somewhat wider than that in Y-direction. This may be due to the spurious radiation from the coaxial probe used for excitation of antenna which is located in X-direction.

The two parameters of importance for obtaining the volume of the tissue absorbing significant amount of power are effective field size (EFS) and penetration depth. The EFS is defined as the area enclosed within the 50 % SAR contour inside the tissue. The penetration depth is the depth at which SAR becomes 1/ e^2 of its value at the surface [15]. The SAR value in muscle is normalized with respect to value at the antenna-muscle interface. The values of EFS and penetration depth are extracted from Fig. 6 and results are given in Table 2. From Table 2 it can be observed that values of EFS and penetration depth in synthetic muscle layer decrease with increase in frequency. The trend of changes in EFS value and penetration depth in synthetic muscle layer may be due to increase in the conductivity of the bio-medium with frequency and frequency dependent characteristics of the antenna. The simulated values of penetration depth in muscle layer are in agreement with measured values. The measured EFS values deviate from the simulated values due to measured resonant frequency not exactly matching with simulated one and also due to error in measurement of position and field strength. Finally, it is noted that maximum simulated value of SAR (10g) are found to be 3.67 W/Kg at the point (-0.292, 0.5, 24.278) for input power of 0.2W, which is above safe level (= 2 W/Kg) for public exposure as per ICNIRP recommendations.

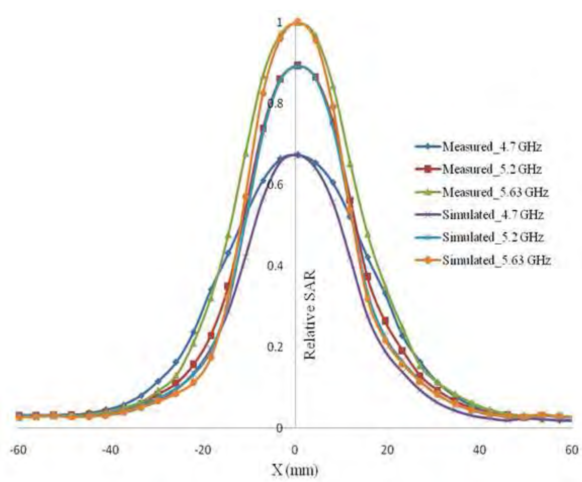

(a)

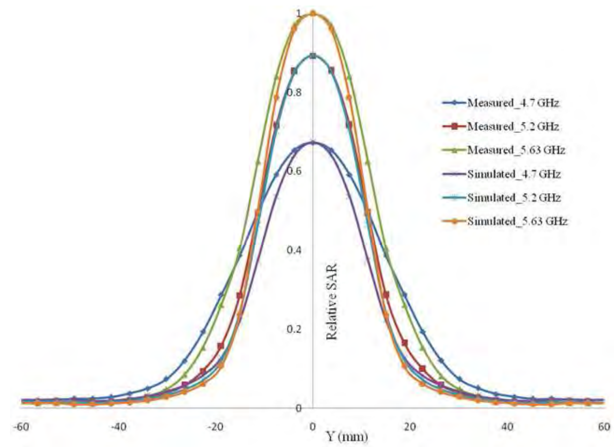

(b)

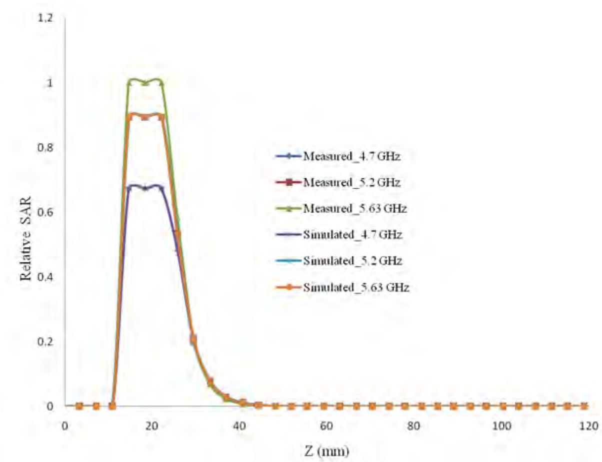

(c)

Fig. 6 Variation of relative SAR in muscle with distance along (a) X- direction, (b) Y-direction, (c) Z-direction

Table 2 SAR performance of DSRDRA in synthetic muscle layer

Parameters	Effective Field Size		Penetration Depth	
	Simulated	Measured	Simulated	Measured
At 4.7 GHz	27.22×24.45 mm^2	37.33×34.01 mm^2	19.89 mm	19.82 mm
At 5.2 GHz	25.50×22.59 mm^2	26.80×24.43 mm^2	19.10 mm	19.14 mm
At 5.63 GHz	24.36×22.64 mm^2	29.3×26.94 mm^2	18.50 mm	18.50 mm

VIII. CONCLUSION

The simulation and experimental studies of SAR distributions in a phantom muscle layer very close to DSDRA have been described. The simulated SAR distribution in muscle has been determined through CST Microwave Studio simulation software and experimental distribution obtained using Agilent make Spectrum Analyzer. The measured results of resonant frequency of the DSRDRA in free space as well as SAR distributions in muscle layer are close to simulated and/or theoretical results. The theoretical return loss bandwidth of DSRDRA in free space is less than the measured and simulated values. This deviation might have occurred due to effect of finite ground plane not considered in theoretical computation. Also, reduction in penetration depth, effective field size and improvement in transverse plane resolution have been noticed with increase in frequency. The results presented here may find potential application in wireless communication and telemedicine fields for designing a wideband ceramic antenna and evaluating the power absorption in a bio-medium due to the antenna. The investigation on the antenna located close to phantom muscle for different antenna-to bio-medium separations may be taken up in future studies.

REFERENCES

[1] Michal Okoniewski, Maria A. Stuchly, "A study of the handset antenna and human body interaction", *IEEE Trans. on Microwave Theory and Techniques*, Vol. 44, no. 10, pp.1855-1864, 1996.

[2] A. Pradier, D. Lautru, M. F. Wong, V. H. Fouad and J. Wiart, "Rigorous evolution of specific absorption rate (SAR) induced in a multilayer biological structure", *European* Microwave Conference, Vol. 3, 2005.

[3] R. K. Mongia and P. Bhartia, "DRA- A review and general design relation for resonant frequency and bandwidth", *International journal of Microwave and Millimeter wave Computer –aided Engineering*, Vol.4, No.3, pp 230-247, 1994.

[4] A. Ittipiboon and R. K. Mongia, "Theoretical and experimental investigations on rectangular dielectric resonator antennas", *IEEE Transactions on Antennas and Propagation*, Vol. 45, No. 9, pp. 1348– 1356, Sept. 1997.

[5] P. Rezaei, M. Hakkak and K. Forooaghi, **"**Design of wideband dielectric resonator antenna with a two segment structure**",** *Progress in Electromagnetics Research*, PIER 66, pp. 111–124, 2006.

[6] Darko Kajfez and A. A. Kishk, "Dielectric Resonator Antenna- Possible Candidate for Adaptive Antenna Arrays", *Proceedings VITEL 2002, International Symposium on Telecommunications, Next Generation Networks and Beyond*, Portoroz, Slovenia, May 13-14, 2002.

[7] M. Saed and R. Yadla, "Microstrip-fed low profile and compact dielectric resonator antennas**",** *Progress In Electromagnetics Research,* PIER 56, pp.151–162, 2006.

[8] Aldo Petosa, "Dielectric Resonator Antennas Handbook*"*, Artech House, Bostonk, london, 2007.

[9] Yuehe Ge, K.P. Esselle "A dielectric resonator antenna for UWB applications", *IEEE International Symposium on Antennas and Propagation Society*, pp.1-4, 1-5 June 2009.

[10] S.H. Zainud-Deen, Emad El-Deen, H.A. Sharshar and M. A. Binyamin, "Design of UMTS dielectric resonator antenna for mobile phone including the biological effects", *Proc. URSI 24th National Radio Science Conference* (NRSC 2007), Faculty of Engineering, Ain Shams Univ., Egypt, pp. C35:1-8, 2007.

[11] T.H. Lee, R.A. Abd-Alhameed and P.S. Excell, "New Dielectric Resonator Antenna Design for Mobile Handsets", URSI-2005. http://rp.iszf.irk.ru/hawk/URSI2005/pdf/BP.10(01068).pdf.

[12] V. K. Palikruru**,** K. Sonoda, R. Surenran and H. Jantunen, "BST-COC composite based rectangular dielectric resonator antenna (DRA) for 2.4-GHz wrist applications", *Progress in Electromagnetics Research C*, Vol. 16, pp. 195-205, 2010.

[13] Ravi Kumar Gangwar, S. P. Singh and D. Kumar, "Wideband dual segment Cylindrical Dielectric Resonator Antenna Terminated in a Bio-medium", *IEEE Microwave Review*, Vol. 16, No. 2, pp. 14-21, December 2010.

[14] Ravi Kumar Gangwar, S.P. Singh and D. Kumar, "Wideband dual segment Rectangular Dielectric Resonator Antenna Terminated in a Bio-medium", *4th International Conference on Communications and Information Technology*, (CIT-2010), Corfu Island, Greece, pp. 64-68, 22-25 July 2010.

[15] Ravi Kumar Gangwar, S. P. Singh and D. Kumar, "SAR distribution in a bio-medium in close proximity with rectangular dielectric resonator antenna", *Progress in Electromagnetic Research B*, Vol. 31, pp. 157-173, 2011.

[16] Ravi Kumar Gangwar, S.P. Singh and D. Kumar, "Modified dual segment Rectangular Dielectric Resonator Antenna Terminated in a Bio-medium*"* *International Journal of Communication, Network and Systems*, Vol. 4, pp. 377-383, 2011.

[17] K. M Luk and K. W. Leung, "Dielectric Resonator Antennas" Research Study Press Hertfordshire, England, UK**,** 2002.

[18] Jian Zhou, Daigoro Hara, and Takehiko Kobayashi, "Development of ultra wideband electromagnetic phantoms for antennas and propagation studies", *First European Conference on Antennas and Propagation (EuCAP 2006)*, pp.1-6, 6-10 Nov.2006 doi: 10.1109/EUCAP.2006.4584884

[19] M. A. Ebrahimi-Ganjeh, "Study of Water Bolus Effect on SAR Penetration Depth and Effective Field Size for Local Hyperthermia", *Progress in Electromagnetics Research*, Vol. 66, pp.111–124, 2006.